NATIONAL ADVISORY COMMITTEE FOR AERONAUTICS

TECHNICAL NOTE

No. 1549

EFFECT OF YAW AT SUPERSONIC SPEEDS ON THEORETICAL AERODYNAMIC COEFFICIENTS OF THIN POINTED WINGS WITH SEVERAL TYPES OF TRAILING EDGE

By W. E. Moeckel

Flight Propulsion Research Laboratory
Cleveland, Ohio

Washington
March 1948

NATIONAL ADVISORY COMMITTEE FOR AERONAUTICS

TECHNICAL NOTE No. 1549

EFFECT OF YAW AT SUPERSONIC SPEEDS ON THEORETICAL AERODYNAMIC COEFFICIENTS OF THIN POINTED WINGS WITH SEVERAL TYPES OF TRAILING EDGE

By W. E. Moeckel

SUMMARY

Expressions are obtained for the aerodynamic coefficients of thin pointed wings with three types of trailing edge. The derivation is based on an equation previously derived for the pressure distribution on a thin yawed delta wing at supersonic speeds. For a semivertex angle of $\tan^{-1} 0.4$, the effect of yaw on the lift coefficient, the wave-drag coefficient, the center of pressure, and the rolling-moment coefficient of a thin pointed wing is compared for three types of trailing edge.

Although the lift coefficient of a pointed wing may be increased by sweeping the trailing edges back from the center line, the variation of center of pressure and rolling moment with yaw angle is thereby increased. The variation of center of pressure and rolling moment with yaw angle is decreased when the trailing edges are swept back from the outer tips of the wing. The chordwise distance from the vertex of a symmetrical pointed wing to its center of pressure was found to be nearly independent of yaw angle for each of the types of trailing-edge sweepback investigated.

INTRODUCTION

Relations are derived in references 1 and 2 for the surface velocity potential of a thin-flat-plate yawed delta wing with leading edges swept behind the Mach cone. From these relations, expressions are obtained for the pressure distribution over the surfaces of the delta wing. For a fixed vertex angle, yaw angle, Mach number, and angle of attack, the pressure coefficient was found to be constant along any radial line from the vertex to the trailing edge. When the pressure coefficient was integrated over the wing surface, explicit expressions were obtained for the lift coefficient and the center of pressure of the delta wing for any yaw angle for which the leading edges remain inside the Mach cone from the vertex.

The results of reference 1 are extended herein to include other types of pointed wing for which the pressure-coefficient equation is the same as for the delta wing. Equations are derived for the aerodynamic coefficients of such wings when the trailing edge is swept back from the outer tips (wing I), swept back from the center (wing II), and swept back from both the center and the outer tips (wing III). The lift coefficient, the wave-drag coefficient, the center of pressure, and the rolling-moment coefficient are evaluated for a semivertex angle of $\tan^{-1} 0.4$ as functions of yaw angle and trailing-edge sweepback angle.

SYMBOLS

The following symbols are used in this report:

C_D	wave-drag coefficient
C_L	lift coefficient
C_l	rolling-moment coefficient
C_p	pressure coefficient
E'	complete elliptic integral of second kind, modulus $\sqrt{1 - G^2}$
F, G	functions of θ_1, Ψ, and β
M	Mach number
S	surface area
U	free-stream velocity
x, y	coordinates parallel and normal to free-stream direction
x_1, y_1	coordinates parallel and normal to wing center line
x_2, y_2	coordinates normal and parallel to trailing edge
x_c	maximum chordwise dimension
x_n	normal distance from vertex to trailing edge
$\bar{x}_1$, $\bar{y}_1$; $\bar{x}_2$, $\bar{y}_2$	coordinates of center of pressure

α angle of attack, radians

$\beta = \sqrt{M^2 - 1}$

Ψ angle of yaw, degrees

θ_1 semiangle of vertex of pointed wing, degrees

θ_2 angle between trailing edge and y_1-axis, degrees

$$\varphi = \tan^{-1}\left(\frac{\tan \theta_1}{2 + \tan \theta_1 \tan \theta_2}\right)$$

$$A_a = \tan \theta_1 + \tan \theta_2 - (1 - \tan \theta_1 \tan \theta_2) \tan(\theta_2 - \varphi)$$

$$A_b = \tan \theta_1 + \tan \theta_2 - (1 - \tan \theta_1 \tan \theta_2) \tan(\theta_2 + \varphi)$$

$$B_a = \tan \theta_1 - \tan \theta_2 + (1 + \tan \theta_1 \tan \theta_2) \tan(\theta_2 - \varphi)$$

$$B_b = \tan \theta_1 - \tan \theta_2 + (1 + \tan \theta_1 \tan \theta_2) \tan(\theta_2 + \varphi)$$

$$a = \frac{\tan \theta_1}{\tan \theta_1 + \tan \Psi}$$

$$a' = \frac{\tan \theta_1}{\tan \theta_1 - \tan \Psi}$$

$$b = \frac{1}{\tan \theta_1 + \tan \Psi}$$

$$b' = \frac{-1}{\tan \theta_1 - \tan \Psi}$$

$$c = a - b \tan \theta_2$$

$$c' = a' - b' \tan \theta_2$$

$$e = a \tan \theta_2 + b$$

$$e' = a' \tan \theta_2 + b'$$

$$H = \frac{2\alpha FK}{r_2 - r_1}$$

I_1, I_2, I_3 definite integrals used in evaluating C_L and center of pressure

$K = \sqrt{\tan(\theta_1 + \Psi) \tan(\theta_1 - \Psi)}$

$K_1 = \dfrac{1}{\sqrt{-ee'}}$

$K_2 = \sqrt{\dfrac{1 - \tan\theta_1 \tan\theta_2}{1 + \tan\theta_1 \tan\theta_2}}$

$K_3 = \sqrt{(c + e\tan\theta_2)(c' + e'\tan\theta_2)}$

$K_4 = \dfrac{ce' + c'e}{2}$

$K_5 = 3 K_4 K_1^2$

$K_6 = K_4 K_5 + cc'$

r integration parameter, y_2/x_2

r_1 lower integration limit

r_2 upper integration limit

Subscripts:

a, b, c, d segments of wing

Ψ evaluated for positive values of Ψ

$-\Psi$ evaluated for negative values of Ψ

ANALYSIS

In the notation of this paper, the equation for the pressure coefficient C_p of a thin delta wing at supersonic speeds, as derived in reference 1, is

$$C_p = -\alpha FK \left[\sqrt{\frac{a + \left(b \frac{y_1}{x_1}\right)}{a' + \left(b' \frac{y_1}{x_1}\right)}} + \sqrt{\frac{a' + \left(b' \frac{y_1}{x_1}\right)}{a + \left(b \frac{y_1}{x_1}\right)}} \right] \qquad (1)$$

where K, a, b, a', and b' are functions of the semivertex angle θ_1 and the yaw angle Ψ, and y_1 and x_1 are coordinates fixed with

respect to the wing. (See fig. 1.) The method used in reference 1 to derive equation (1) was approximate. The approximation, however, affected only the values of the factor F. An exact expression for F has been obtained in reference 2. In the notation used herein, this expression is

$$F = \frac{1}{E'} \sqrt{\frac{2G}{\beta \left[\tan (\theta_1 + \Psi) + \tan (\theta_1 - \Psi)\right]}} \qquad (2)$$

where

$$G = \frac{1+\beta^2\tan(\theta_1+\Psi)\tan(\theta_1-\Psi) - \sqrt{\left[1-\beta^2\tan^2(\theta_1+\Psi)\right]\left[1-\beta^2\tan^2(\theta_1-\Psi)\right]}}{\beta\left[\tan (\theta_1 + \Psi) + \tan (\theta_1 - \Psi)\right]}$$

Values of F for several values of θ_1 and for two values of β are shown in figure 2. A plot of the variation of pressure coefficient with yaw angle Ψ over a wing with semivertex angle of $\tan^{-1} 0.4$ is shown in figure 3, which is taken from figure 6 of reference 1. (The use of equation (2) in place of the approximate values of F had no noticeable effect on the values shown in fig. 3.)

Because C_p is constant along a given line from the vertex, equation (1) is also valid for the types of wing shown in figure 4 provided that the leading edges fall behind the Mach waves from the vertex and the trailing edges fall ahead of the Mach waves from the foremost points of the trailing edges. These conditions may be written as

$$\theta_1 + \Psi \leq \cot^{-1} \beta \qquad (3)$$

$$\theta_2 + \Psi \leq 90^\circ - \cot^{-1} \beta \qquad (3a)$$

Equations (3) and (3a) imply that

$$\theta_1 + \theta_2 + 2\Psi \leq 90^\circ \qquad (3b)$$

In order to simplify the integrations required to determine lift coefficient and center of pressure, it is convenient to obtain equation (1) in terms of coordinate axes parallel and perpendicular to the trailing edge (fig. 4). With this coordinate system, the integration need be performed for only one variable and the x_2 coordinate of the center of pressure is constant ($\bar{x}_2 = 2x_n/3$).

$$x_1 = x_2 \cos \theta_2 + y_2 \sin \theta_2 \tag{4}$$

$$y_1 = y_2 \cos \theta_2 - x_2 \sin \theta_2 \tag{4a}$$

$$\frac{y_1}{x_1} = \frac{\frac{y_2}{x_2} - \tan \theta_2}{1 + \frac{y_2}{x_2} \tan \theta_2} \tag{4b}$$

When equation (4b) is substituted into equation (1), the following expression is obtained for the pressure coefficient:

$$C_p = -\alpha FK \left(\sqrt{\frac{c + er}{c' + e'r}} + \sqrt{\frac{c' + e'r}{c + er}} \right)$$

$$= -\alpha FK \left[\frac{(c + c') + (e + e')r}{\sqrt{(c + er)\ (c' + e'r)}} \right] \tag{5}$$

where $r = y_2/x_2$. The lift coefficient and the center of pressure are then obtainable from the following equations:

$$C_L = \frac{-2 \int C_p dS}{\int dS} = \frac{-2 \int_{r_1}^{r_2} C_p dr}{r_2 - r_1} = \frac{2\alpha FK}{r_2 - r_1} \left[(c+c') \int_{r_1}^{r_2} \frac{dr}{\sqrt{(c+er)\ (c'+e'r)}} \right.$$

$$\left. + (e+e') \int_{r_1}^{r_2} \frac{r dr}{\sqrt{(c+er)(c'+e'r)}} \right] \tag{6}$$

$$\frac{\bar{y}_2}{x_2} = \frac{\int_{r_1}^{r_2} C_p r dr}{\int_{r_1}^{r_2} C_p dr} = \frac{2\alpha FK}{C_L(r_2 - r_1)} \left[(c+c') \int_{r_1}^{r_2} \frac{r dr}{\sqrt{(c+er)(c'+e'r)}} \right.$$

$$\left. + (e+e') \int_{r_1}^{r_2} \frac{r^2\, dr}{\sqrt{(c+er)(c'+e'r)}} \right] \tag{7}$$

Because the definite integrals in equations (6) and (7) occur for each of the wings, these equations are written in the following form:

$$C_L = H\left[(c + c')\, I_1 + (e + e')\, I_2\right] \tag{6a}$$

$$\frac{\bar{y}_2}{\bar{x}_2} = \frac{H}{C_L}\left[(c + c')\, I_2 + (e + e')\, I_3\right] \tag{7a}$$

where

$$I_1 = \frac{2}{\sqrt{-ee'}}\left[\tan^{-1}\sqrt{\frac{-e'\,(c + er)}{e\,(c' + e'r)}}\right]_{r_1}^{r_2} \tag{8}$$

$$I_2 = \frac{1}{ee'}\left\{\left[\sqrt{(c + er)(c' + e'r)}\right]_{r_1}^{r_2} - \left(\frac{ce' + c'e}{2}\right) I_1\right\} \tag{9}$$

$$I_3 = \frac{1}{2ee'}\left\{\left[\sqrt{(c + er)(c' + e'r)}\left(r - \frac{3(ce' + c'e)}{2ee'}\right)\right]_{r_1}^{r_2} + I_1\left[\frac{3(ce' + c'e)^2}{4ee'} - cc'\right]\right\} \tag{10}$$

$$\bar{x}_2 = \frac{2}{3}\, x_n \tag{11}$$

In order to obtain the lift coefficient and the center of pressure for the wings of figure 4, it remains only to evaluate I_1, I_2, and I_3 for the proper integration limits for each wing. The expressions for the quantities to be used in equations (6a) and (7a) are summarized for each wing in table I. The limits r_2 and r_1 may be found in the expressions given for H/α.

For wings I and II, the expressions in table I are the same for either half of the wing. The lift coefficient for the unshaded half in figure 4(a) or 4(b) is obtained when Ψ is replaced by $-\Psi$ in calculating the values of $c + c'$ and $e + e'$ in equation (6a). The lift coefficient for the entire wings is one-half the sum of the lift coefficients of the two halves; that is,

$$C_L = \frac{1}{2}\left[(C_{L,a})_{\Psi} + (C_{L,a})_{-\Psi}\right] \tag{12}$$

where $(C_{L,a})_{-\Psi}$ is the lift coefficient obtained from equation (6a) when $-\Psi$ is substituted for Ψ in the terms $c + c'$ and $e + e'$. Thus by carrying out the integrations over half of the wing surface and calculating the lift coefficient for negative as well as positive values of Ψ, the lift coefficient of the entire wing may be obtained.

Coordinates of the center of pressure for the entire wing are similarly obtained from values computed for only one-half of the wing by reconverting the coordinates obtained from equation (7a) to the x_1, y_1 coordinate system. Then, for the entire wing (figs. 4(a) and 4(b)),

$$\bar{y}_1 = \frac{(C_{L,a}\,\bar{y}_{1,a})_{\Psi} - (C_{L,a}\,\bar{y}_{1,a})_{-\Psi}}{(C_{L,a})_{\Psi} + (C_{L,a})_{-\Psi}} \tag{13}$$

$$\bar{x}_1 = \frac{(C_{L,a}\,\bar{x}_{1,a})_{\Psi} + (C_{L,a}\,\bar{x}_{1,a})_{-\Psi}}{(C_{L,a})_{\Psi} + (C_{L,a})_{-\Psi}} \tag{13a}$$

For the wing of figure 4(c), the expressions in table I pertain to the segments a and b. The lift coefficients for each half of the wing are the mean of the coefficients of the two segments weighted according to the areas of the segments; that is

$$C_{L,a+c} = \frac{S_a(C_{L,a})_{\Psi} + S_b(C_{L,b})_{-\Psi}}{S_a + S_b} \tag{14}$$

$$C_{L,b+d} = \frac{S_a(C_{L,a})_{-\Psi} + S_b(C_{L,b})_{\Psi}}{S_a + S_b} \tag{14a}$$

The coordinates of the centers of pressure for each half of the wing are:

$$\bar{y}_{1,a+c} = \frac{S_a(C_{L,a}\,\bar{y}_{1,a})_{\Psi} - S_b(C_{L,b}\,\bar{y}_{1,b})_{-\Psi}}{S_a(C_{L,a})_{\Psi} + S_b(C_{L,b})_{-\Psi}} \tag{15}$$

$$\bar{x}_{1,a+c} = \frac{S_a(C_{L,a}\,\bar{x}_{1,a})_{\Psi} + S_b(C_{L,b}\,\bar{x}_{1,b})_{-\Psi}}{S_a(C_{L,a})_{\Psi} + S_b(C_{L,b})_{-\Psi}} \tag{15a}$$

$$\bar{y}_{1,b+d} = \frac{-S_a(C_{L,a}\,\bar{y}_{1,a})_{-\Psi} + S_b(C_{L,b}\,\bar{y}_{1,b})_{\Psi}}{S_a(C_{L,a})_{-\Psi} + S_b(C_{L,b})_{\Psi}} \tag{16}$$

$$\bar{x}_{1,b+d} = \frac{S_a(C_{L,a}\,\bar{x}_{1,a})_{-\Psi} + S_b(C_{L,b}\,\bar{x}_{1,b})_{\Psi}}{S_a(C_{L,a})_{-\Psi} + S_b(C_{L,b})_{\Psi}} \tag{16a}$$

where

$$S_a = \frac{x_{n,a}^2}{2}\left[\tan(\theta_2 - \varphi) - \tan(\theta_2 - \theta_1)\right] \tag{17}$$

$$S_b = \frac{x_{n,b}^2}{2}\left[\tan(\theta_2 + \varphi) - \tan\theta_2\right] \tag{17a}$$

In order to obtain the lift coefficient and the center of pressure for the entire wing, the values obtained for each half are combined as in equations (12) and (13). For $\theta_2 = 0$, the equations for the lift coefficient and for the center of pressure for all three wings reduce to those obtained for the delta wing in reference 1; that is,

$$C_L = \frac{2\pi\alpha F \tan\theta_1}{\sqrt{1 - \tan^2\theta_1 \tan^2\Psi}} \tag{18}$$

$$\frac{\bar{y}_1}{\bar{x}_1} = -\frac{\tan\Psi}{2} \tag{19}$$

$$\bar{x}_1 = \frac{2}{3}x_c \tag{19a}$$

RESULTS

The results of computations for pointed wings having a semivertex angle of $\theta_1 = \tan^{-1} 0.4 = 21.8^{\circ}$ are presented in figures 5 to 7.

The lift-slope curves (which are also the drag-slope curves divided by α, if leading-edge suction is neglected, because $C_D/C_L = \alpha$ for the flat-plate wing) are plotted in figure 5 as functions of yaw angle and trailing-edge sweepback angle for a Mach number of $\sqrt{2}$. Results are presented for half of each wing and for the entire wing. The variation of lift coefficient with yaw angle is similar for each of the three wings considered. As the trailing-edge sweepback angle θ_2 is increased, the lift coefficient decreases for wings I and III, but increases for wing II. These results are to be expected because, as shown in figure 3, the pressure distribution is assymptotic to the outer edges of the wing. Hence, removing portions of the wing from the outer edges should lower the lift coefficient. The variation of lift coefficient with θ_2 is slightly greater for wing III than for wing I.

The variation of the center of pressure with yaw angle and trailing-edge sweepback angle is shown in figure 6 for the wings of figure 4. Because the factor F, which is the only quantity that varies with Mach number, cancels in the calculations of center of pressure, these results are valid for all Mach numbers so long as the conditions of equations (3) and (3a) are fulfilled. The variation of center of pressure with yaw angle is shown for one-half of each wing as well as for the entire wing. The results for one-half of each wing, of course, have significance only as an aid in computing the results for the entire wing. For halves of wings I and II, the center of pressure moves along lines parallel to the trailing edge as the yaw angle is varied. For half of wing III, the $\bar{x}_1$ coordinate of the center of pressure is only slightly dependent on the yaw angle.

For the complete wings I, II, and III, the $\bar{x}_1$ coordinate of the center of pressure remains constant as Ψ is varied. For fixed values of Ψ, the center of pressure for each of the wings moves along straight lines as θ_2 is varied. In particular, for wing I (fig. 6(b)) the lines for fixed values of Ψ are inclined at the angle Ψ to the center line and appear to intersect at a common point whose coordinates are $\bar{y}_1 = 0$, $\bar{x}_1 = x_c/3$. Hence, the approximate equation for the variation of center of pressure with yaw angle for this wing is

$$\frac{\bar{y}_1}{x_c} = \tan \Psi \left(\frac{\bar{x}_1}{x_c} - \frac{1}{3} \right) \tag{20}$$

For wings II and III, the center of pressure for fixed values of Ψ moves along lines that appear to have a common intersection point at the coordinates $\bar{y}_1 = 0$, $\bar{x}_1 = 1.43\ x_c$ and $\bar{y}_1 = 0$, $\bar{x}_1 = 0.473\ x_c$, respectively. For these two wings, however, the lines are not inclined at the angle Ψ with respect to the $\bar{x}_1/x_c$ axis. The reasons for common intersection points are not obvious from the equations for the center of pressure and these intersections may be only apparent, that is, only true within the accuracy of the plots.

The intersections of the constant θ_2 lines for halves of wings I and II at the coordinates $\bar{y}_1 = 0$, $\bar{x}_1 = 2x_c/3$ and $\bar{y}_1 = 0.4\bar{x}_1$, $\bar{x}_1 = 2x_c/3$, respectively, also have no readily discernible reason although a common intersection point is plausible because each of these lines must be parallel to the trailing edge. (The constant θ_2 lines are parallel to the trailing edges because the center of pressure for each elementary area of the half-wings lies 2/3 of the distance from the vertex to the trailing edge.)

A comparison of figures 6(b), 6(d), and 6(f) shows that the center of pressure varies considerably more with yaw angle for wing II than for wings I and III. This result is to be expected because the pressure is highest along the edges of the wings and least near the center. (See fig. 3.) Removing portions along the outer edges should therefore reduce the center-of-pressure travel. The lift coefficient, of course, was also less for wings I and III.

The variation of the rolling-moment coefficient with yaw angle and trailing-edge sweepback angle is shown for wings I and II in figure 7. This coefficient is defined by the equation

$$C_l = C_L \frac{\bar{y}_1}{x_c}$$

and is a measure of the rolling moment about the center line of the entire wing. For wing I the variation of C_l with yaw angle is less than for wing II. The variation of rolling-moment coefficient with yaw angle and θ_2 was almost the same for wing III as for wing I because the lift coefficient is slightly smaller and the center-of-pressure travel slightly greater for wing III than for wing I.

Because the $\bar{x}_1$ coordinate of the center of pressure remains constant for each of the wings for a given θ_2, no change in pitching moment with yaw angle need be expected under steady-state conditions for any of the wings considered if the center of gravity is on the center-of-pressure line obtained for $\Psi = 0$.

CONCLUSIONS

From calculations of the variation of aerodynamic coefficients of pointed wings with yaw angle and trailing-edge sweepback angle, the following conclusions may be drawn:

1. The lift coefficient of a pointed wing may be increased by sweeping the trailing edges back from the center line.

2. The chordwise distance from the vertex of a symmetrical pointed wing to the center of pressure is nearly independent of yaw angle for any of the types of trailing-edge sweepback investigated.

3. The variation of center of pressure with yaw angle is decreased when the trailing edges are swept back from the outer tips and is increased when the trailing edges are swept back from the center line.

4. The variation of rolling-moment coefficient with yaw angle for a pointed wing may be reduced by sweeping the trailing edges back from the outer tips.

Flight Propulsion Research Laboratory,
National Advisory Committee for Aeronautics,
Cleveland, Ohio, October 30, 1947.

REFERENCES

1. Evvard, John C.: The Effects of Yawing Thin Pointed Wings at Supersonic Speeds. NACA TN No. 1429, 1947.

2. Heaslet, Max. A., Lomax, Harvard, and Jones, Arthur L.: Volterra's Method for Three-Dimensional Supersonic Flow. NACA TN No. 1412, 1947.

TABLE I. - VALUES REQUIRED TO OBTAIN LIFT COEFFICIENT AND CENTER OF PRESSURE FOR WINGS OF FIGURE 4

	Wing I, segment a	Wing II, segment a	Wing III, segment a	Wing III, segment b
$\frac{H}{a}$	$\frac{2FK}{\tan\theta_2 - \tan(\theta_2-\theta_1)}$	$\frac{2FK}{\tan(\theta_2+\theta_1) - \tan\theta_2}$	$\frac{2FK}{\tan(\theta_2-\varphi) - \tan(\theta_2-\theta_1)}$	$\frac{2FK}{\tan(\theta_2+\varphi) - \tan\theta_2}$
I_1	$2K_1 \tan^{-1} K_2$	$2K_1\left(\frac{\pi}{2} - \tan^{-1} K_2\right)$	$2K_1\left[\tan^{-1}\left(K_2\sqrt{\frac{B_a}{A_a}}\right)\right]$	$2K_1\left[\tan^{-1}\left(K_2\sqrt{\frac{B_b}{A_b}}\right) - \tan^{-1} K_2\right]$
I_2	$-K_1^2\left(K_3 - K_4 I_1\right)$	$K_1^2\left(K_3 + K_4 I_1\right)$	$-K_1^2\left(\sqrt{\frac{A_aB_a}{\tan^2\theta_1 - \tan^2\psi}} - K_4 I_1\right)$	$-K_1^2\left(\sqrt{\frac{A_aB_a}{\tan^2\theta_1 - \tan^2\psi}} - K_3 - K_4 I_1\right)$
I_3	$-\frac{K_1^2}{2}\left[K_3\left(\tan\theta_2 + K_5\right) - K_6 I_1\right]$	$\frac{K_1^2}{2}\left[K_3\left(\tan\theta_2 + K_5\right) + K_6 I_1\right]$	$-\frac{K_1^2}{2}\left\{\sqrt{\frac{A_aB_a}{\tan^2\theta_1 - \tan^2\psi}}\left[\tan(\theta_2-\varphi) + K_5\right] - K_6 I_1\right\}$	$-\frac{K_1^2}{2}\left\{\sqrt{\frac{A_bB_b}{\tan^2\theta_1 - \tan^2\psi}}\left[\tan(\theta_2+\varphi) + K_5\right] - K_3\left[\tan\theta_2 + K_5\right] - K_6 I_1\right\}$
$\frac{x_n}{x_c}$	$\cos\theta_2$	$\frac{\cos(\theta_2+\theta_1)}{\cos\theta_1}$	$\frac{\cos(\theta_2-\varphi)}{\cos\varphi}$	$\frac{\cos(\theta_2+\varphi)}{\cos\varphi}$

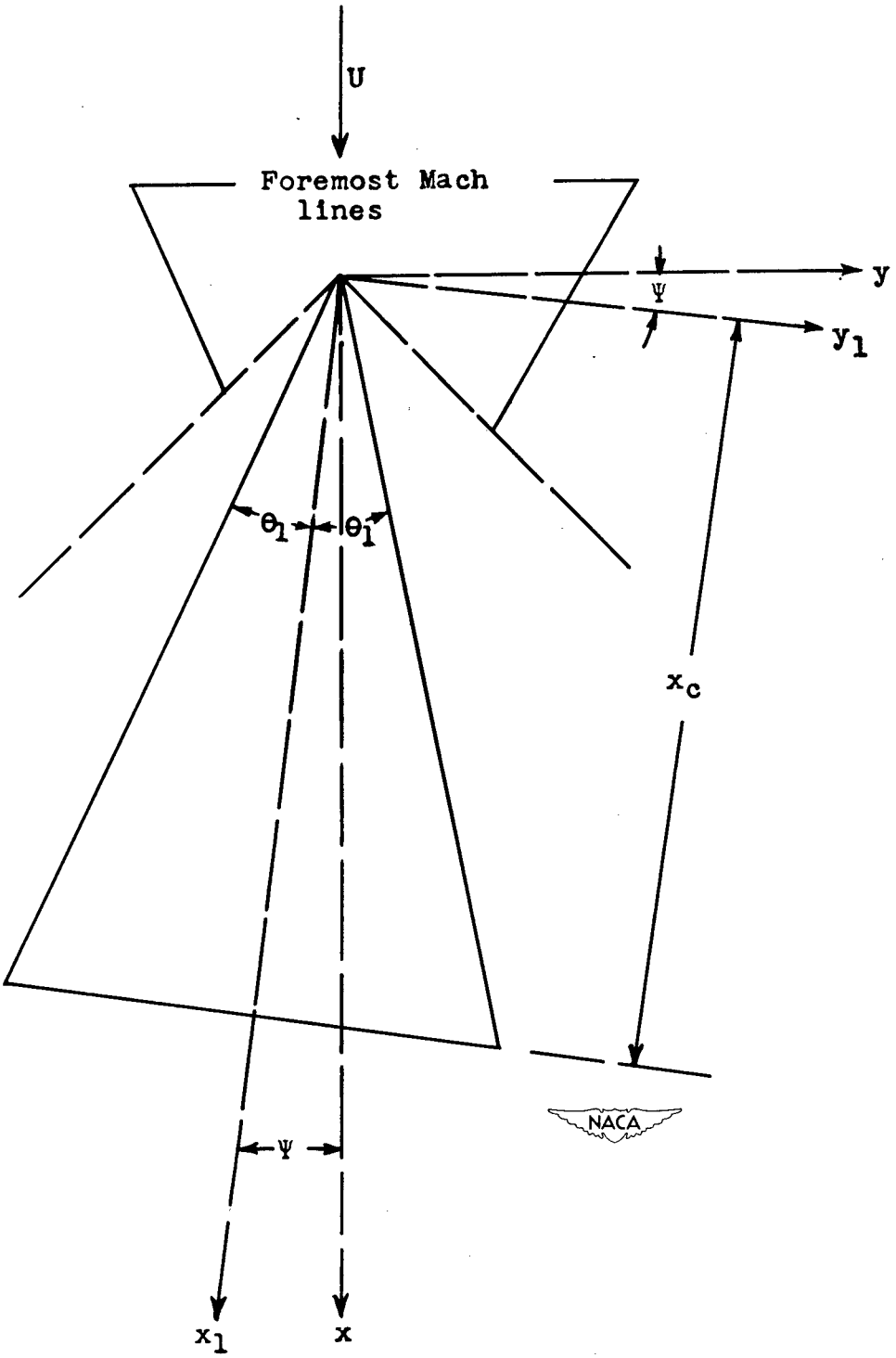

Figure 1. - Coordinates for yawed delta wing.

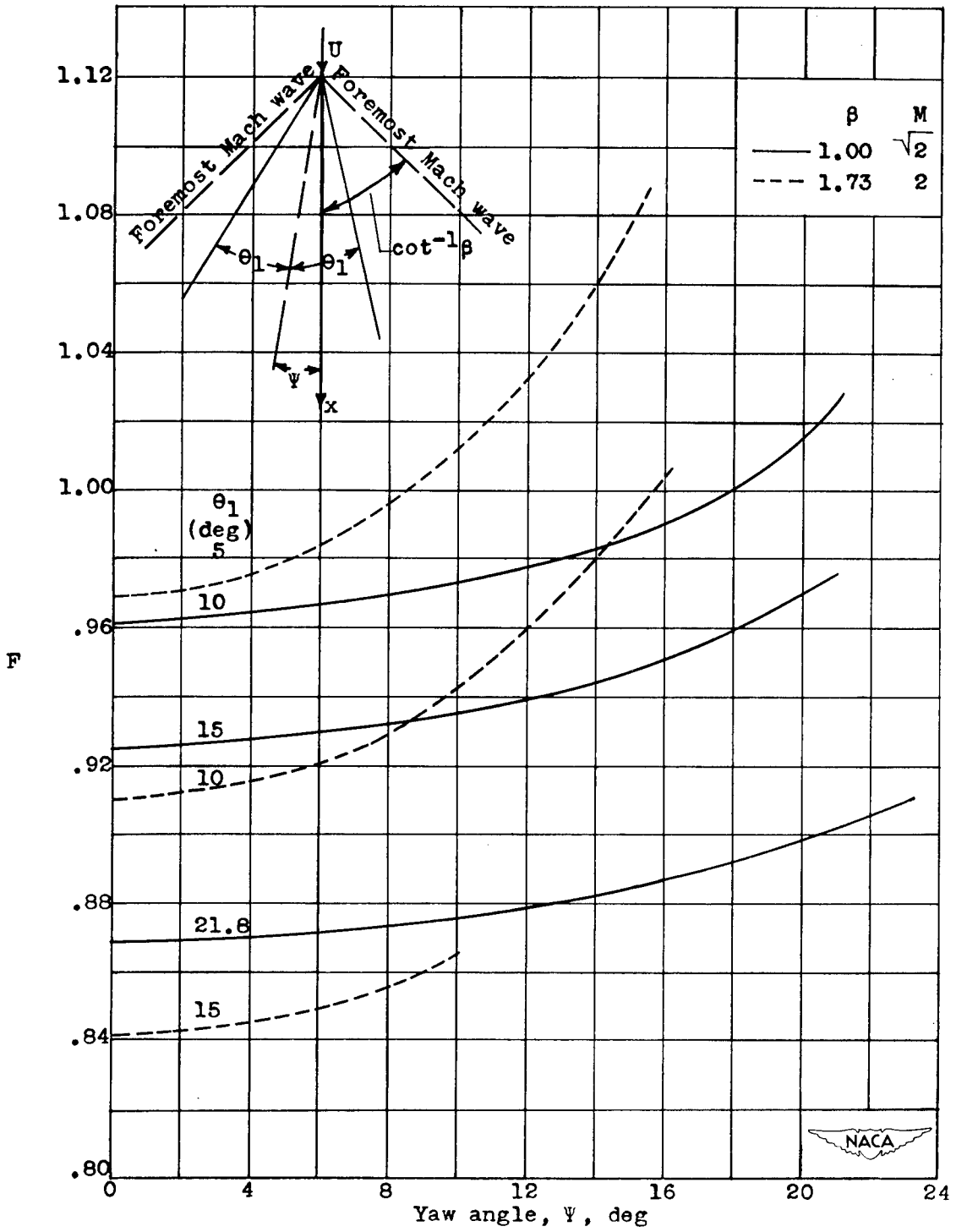

Figure 2. - Variation of F with yaw angle and vertex angle for two Mach numbers.

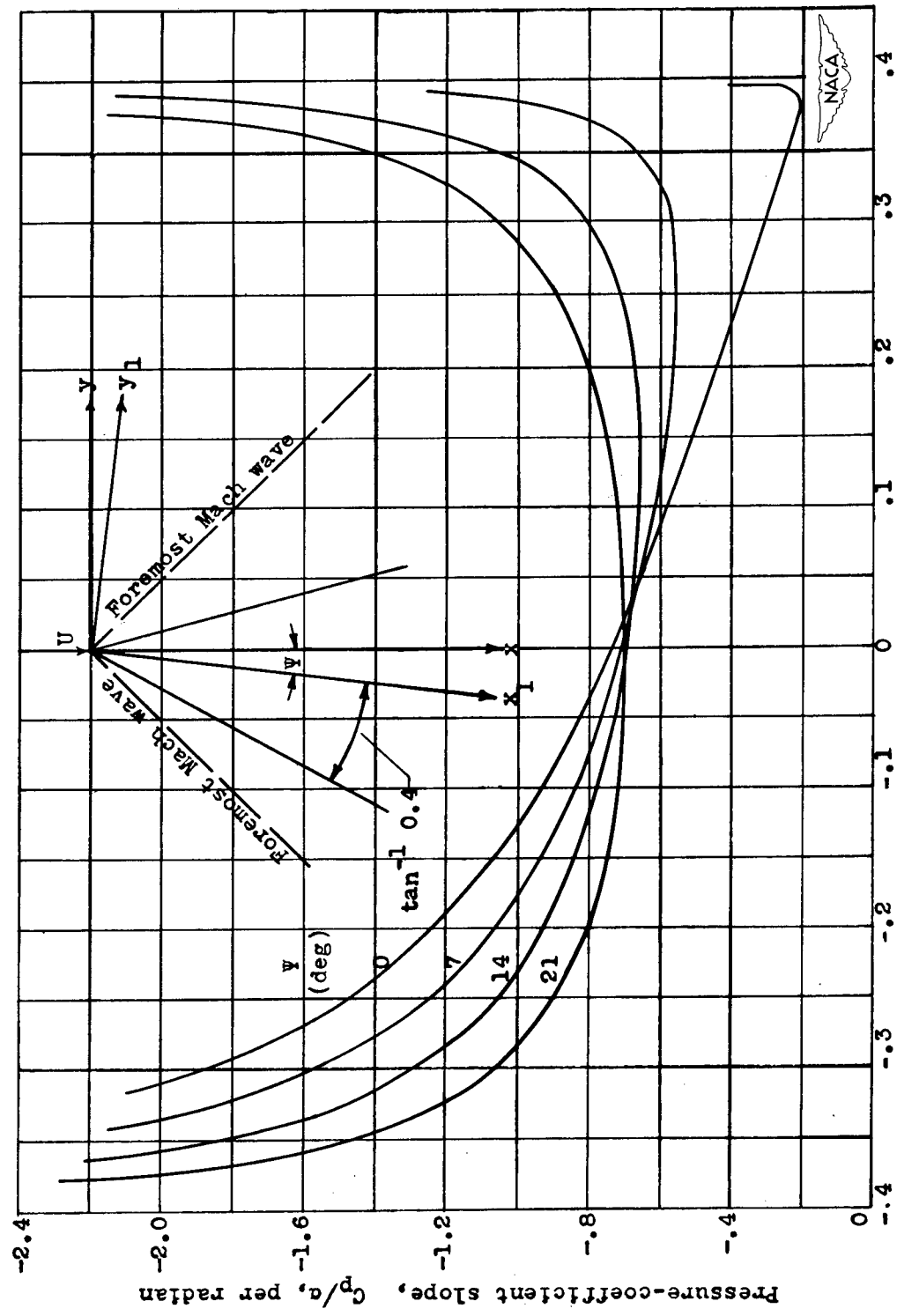

Figure 3. - Variation of pressure-coefficient distribution with yaw angle for thin pointed wing. $\theta_1 = \tan^{-1} 0.4$; $M = \sqrt{2}$. (From fig. 6 of reference 1.)

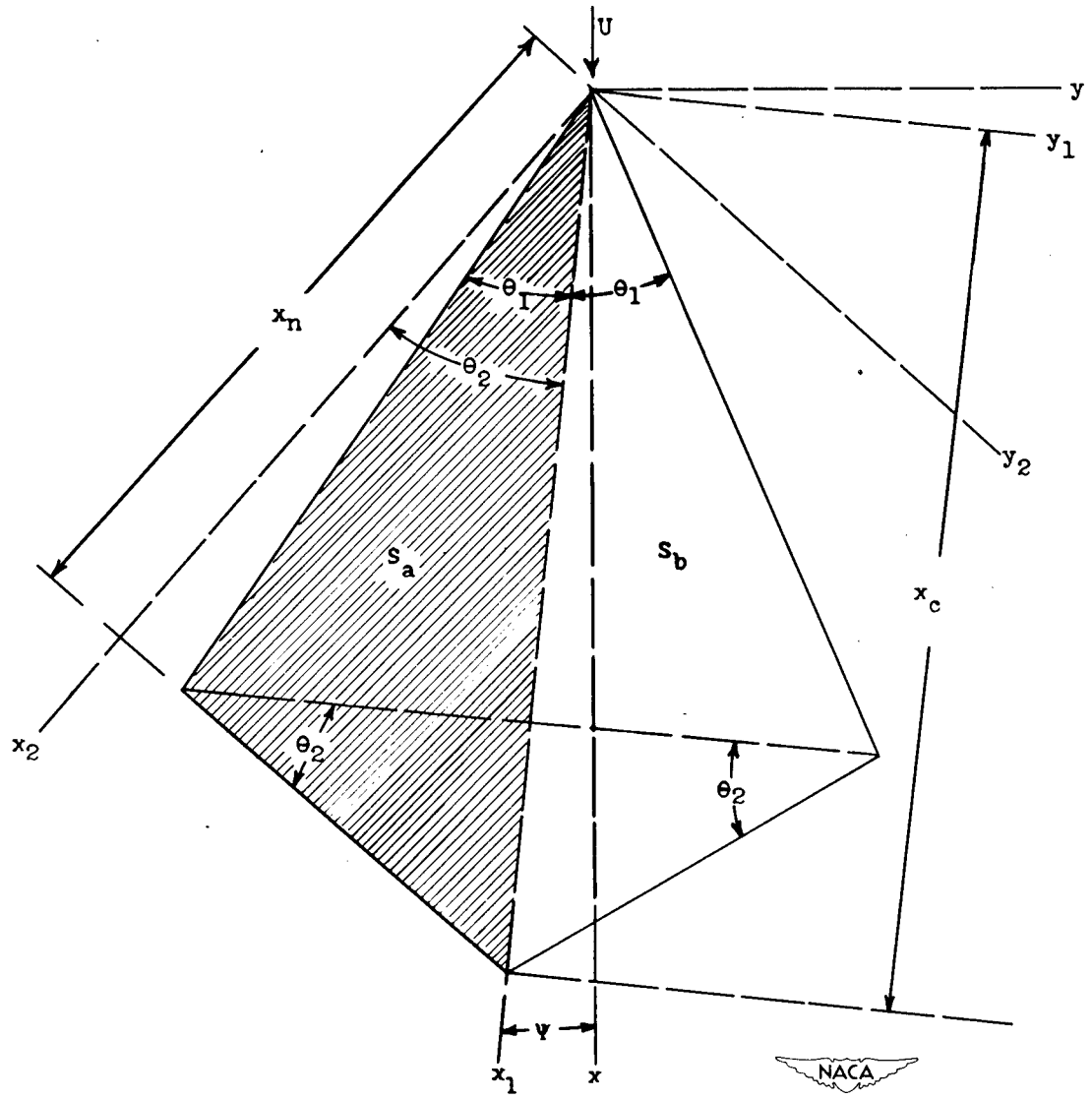

(a) Wing I; trailing edges swept back from outer tips.

Figure 4. - Geometric parameters for pointed wings with swept-back trailing edges. (Equations in table I apply to shaded areas.)

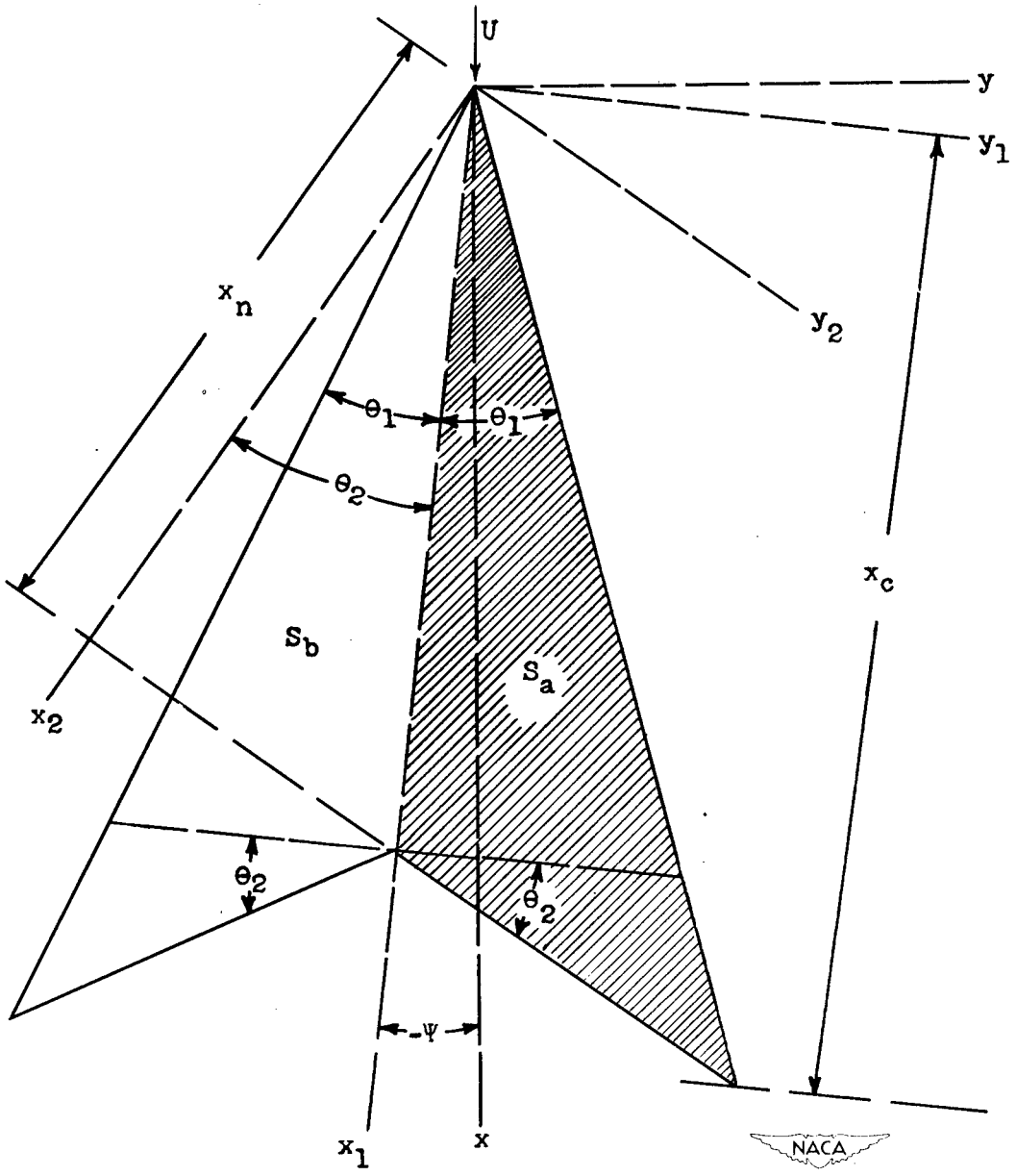

(b) Wing II; trailing edges swept back from center.

Figure 4. Continued. Geometric parameters for pointed wings with swept-back trailing edges. (Equations in table I apply to shaded areas.)

848

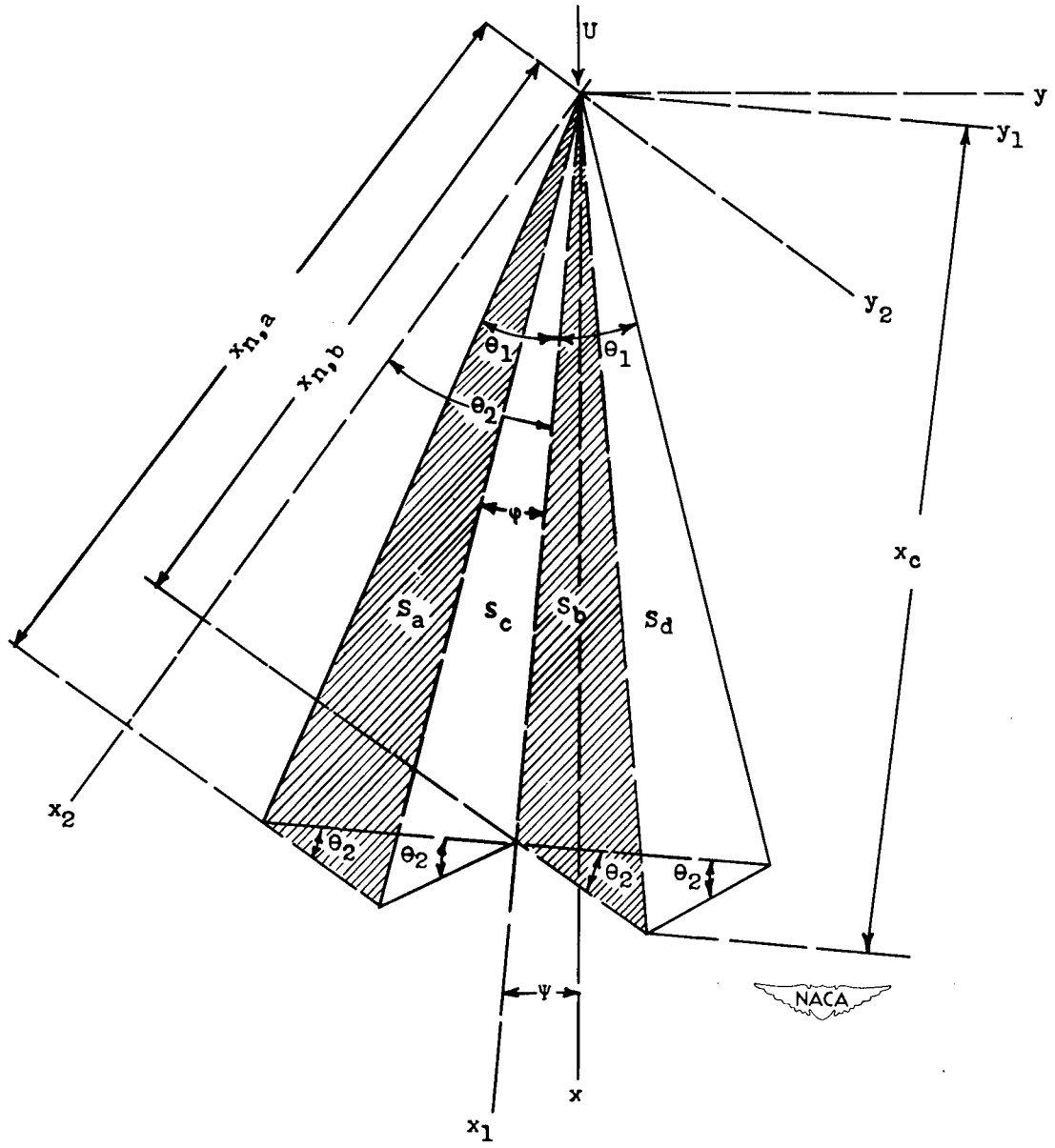

(c) Wing III; trailing edges swept back from center and outer tips.

Figure 4. – Concluded. Geometric parameters for pointed wings with swept-back trailing edges. (Equations in table I apply to shaded areas.)

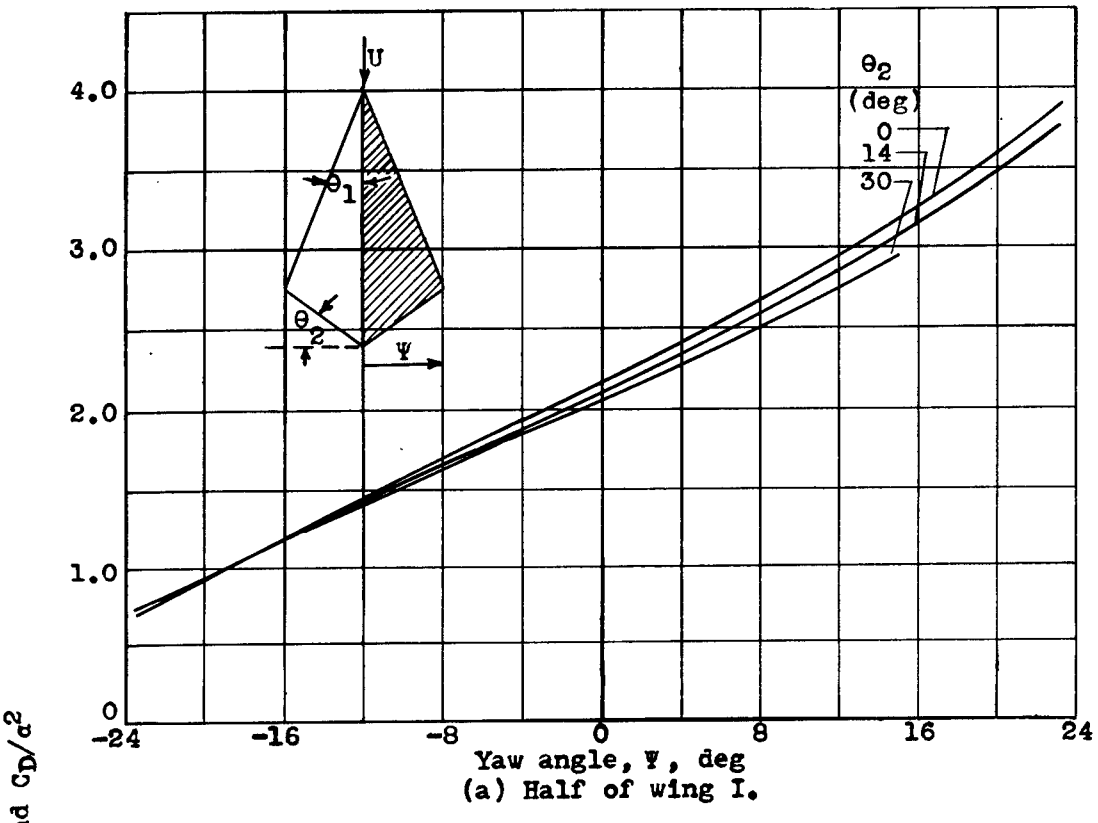

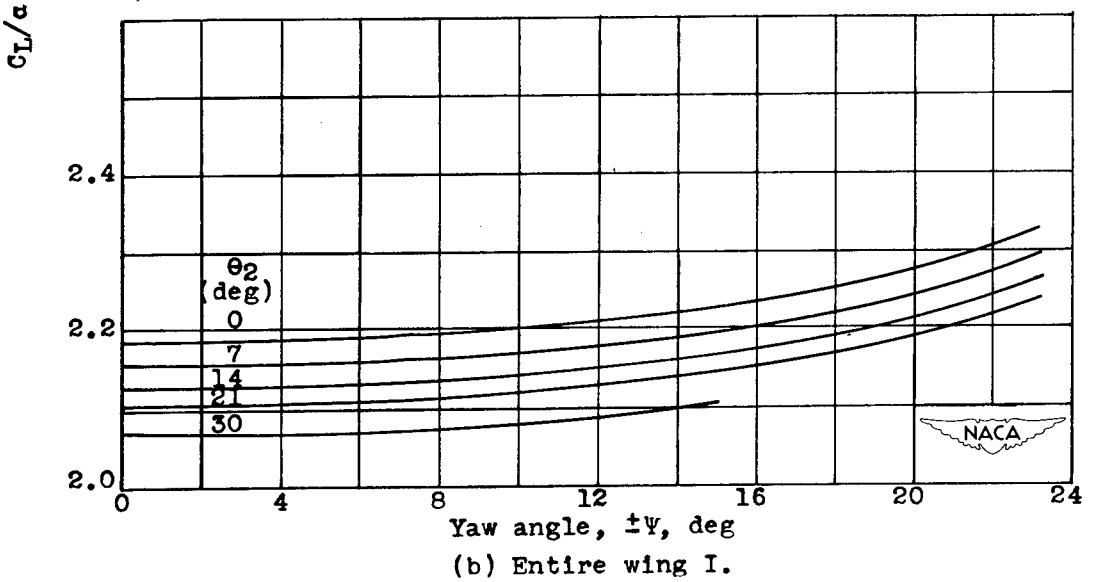

Figure 5. - Lift and drag coefficients as function of yaw angle and trailing-edge sweepback angle θ_2. $\theta_1 = \tan^{-1} 0.4$; $M = \sqrt{2}$.

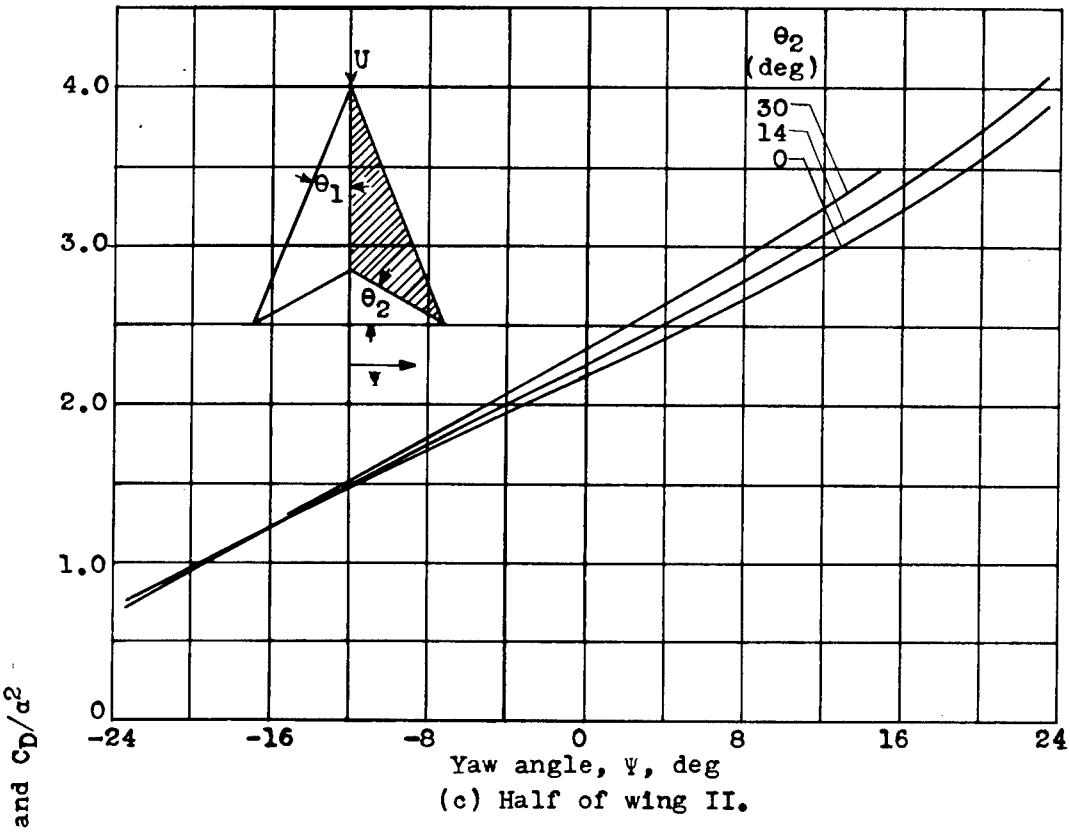

(c) Half of wing II.

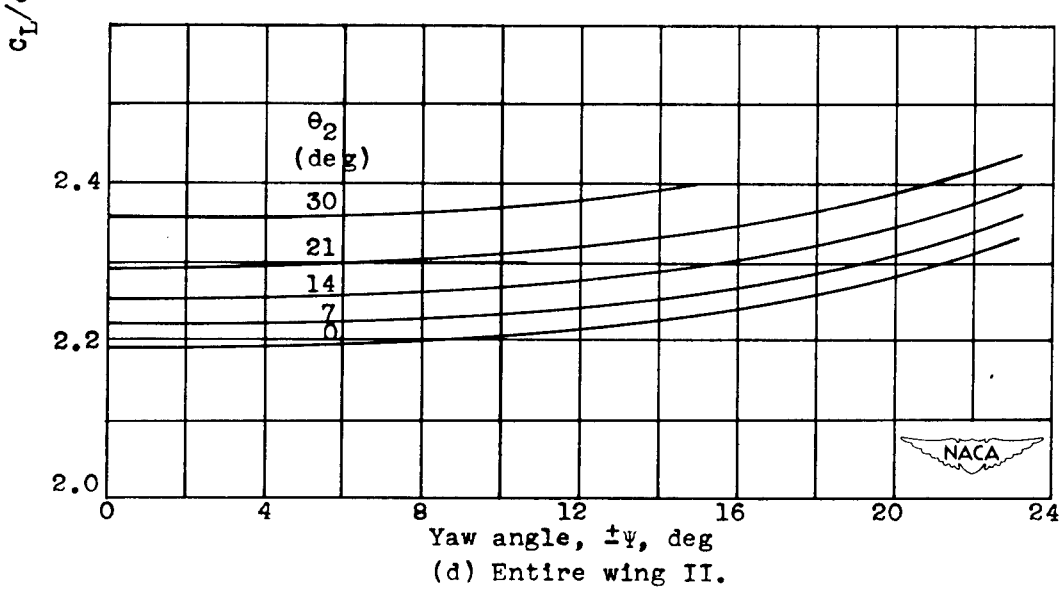

(d) Entire wing II.

Figure 5. - Continued. Lift and drag coefficients as function of yaw angle and trailing-edge sweepback angle θ_2. $\theta_1 = \tan^{-1} 0.4$; $M = \sqrt{2}$.

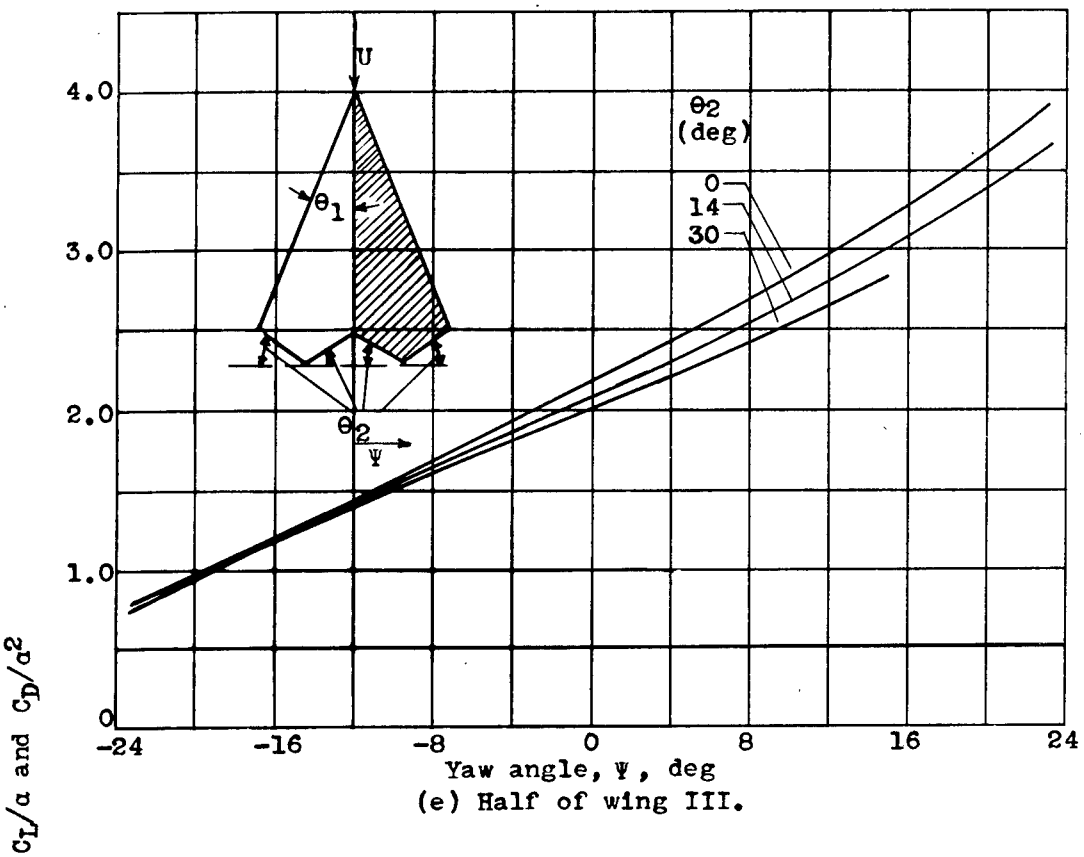

(e) Half of wing III.

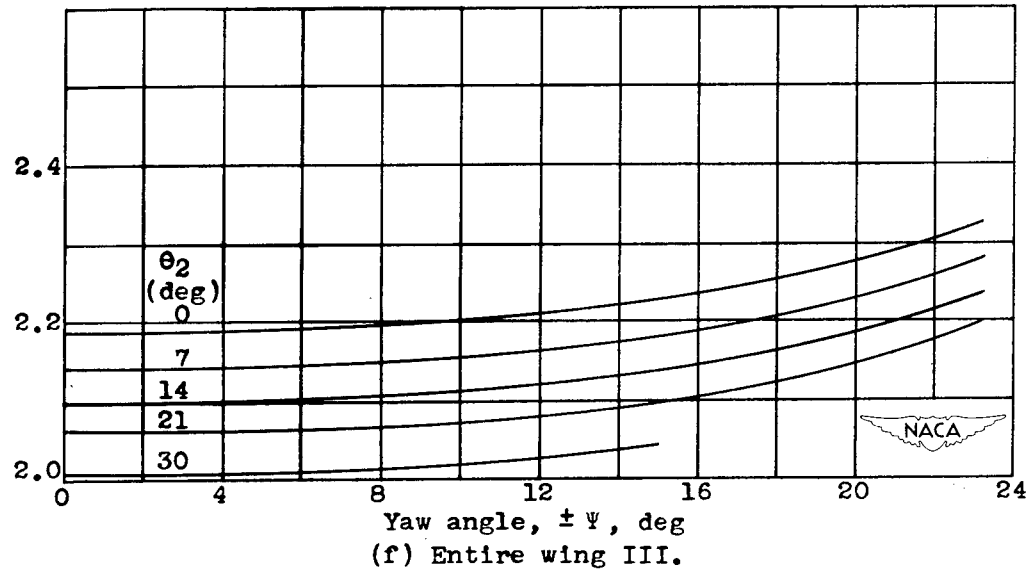

(f) Entire wing III.

Figure 5. - Concluded. Lift and drag coefficients as function of yaw angle and trailing-edge sweepback angle θ_2. $\theta_1 = \tan^{-1} 0.4$; $M = \sqrt{2}$.

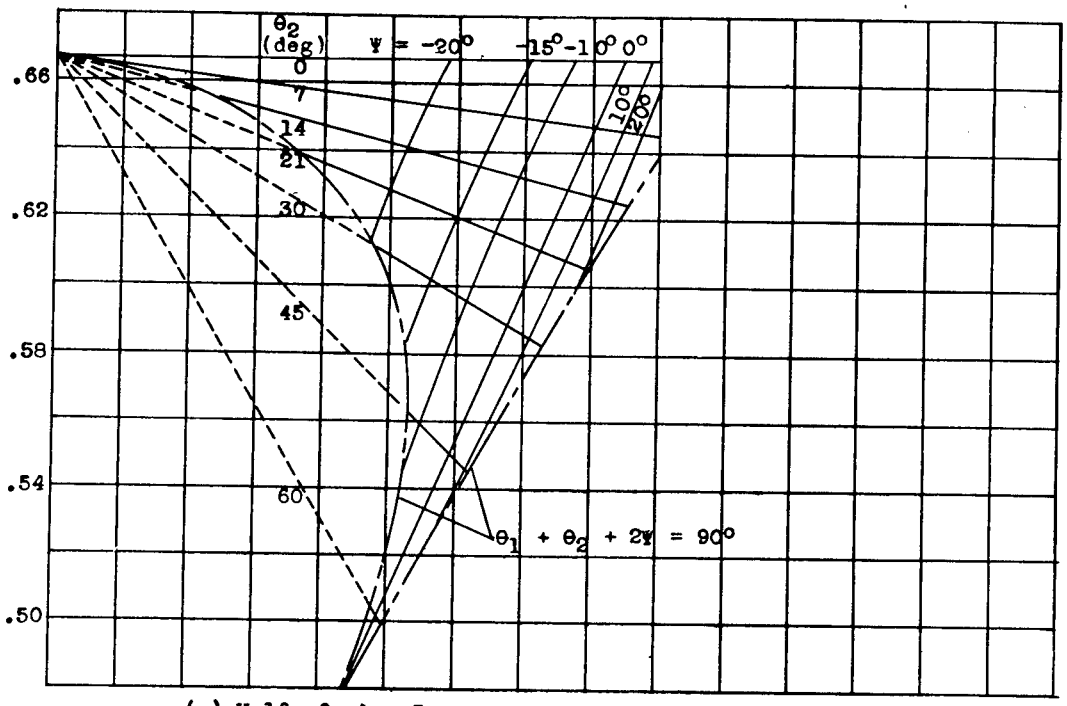

(a) Half of wing I.

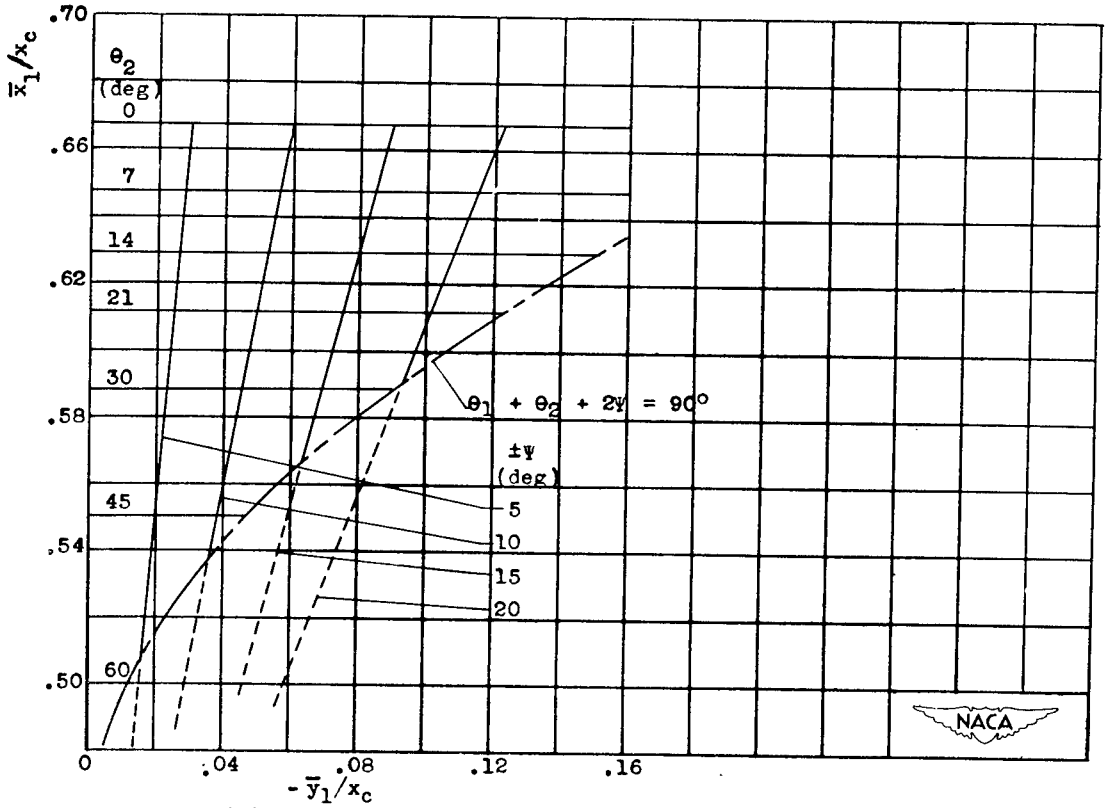

(b) Entire wing I.

Figure 6. - Variation of center of pressure with yaw angle and trailing-edge sweepback angle. $\theta_1 = \tan^{-1} 0.4$.

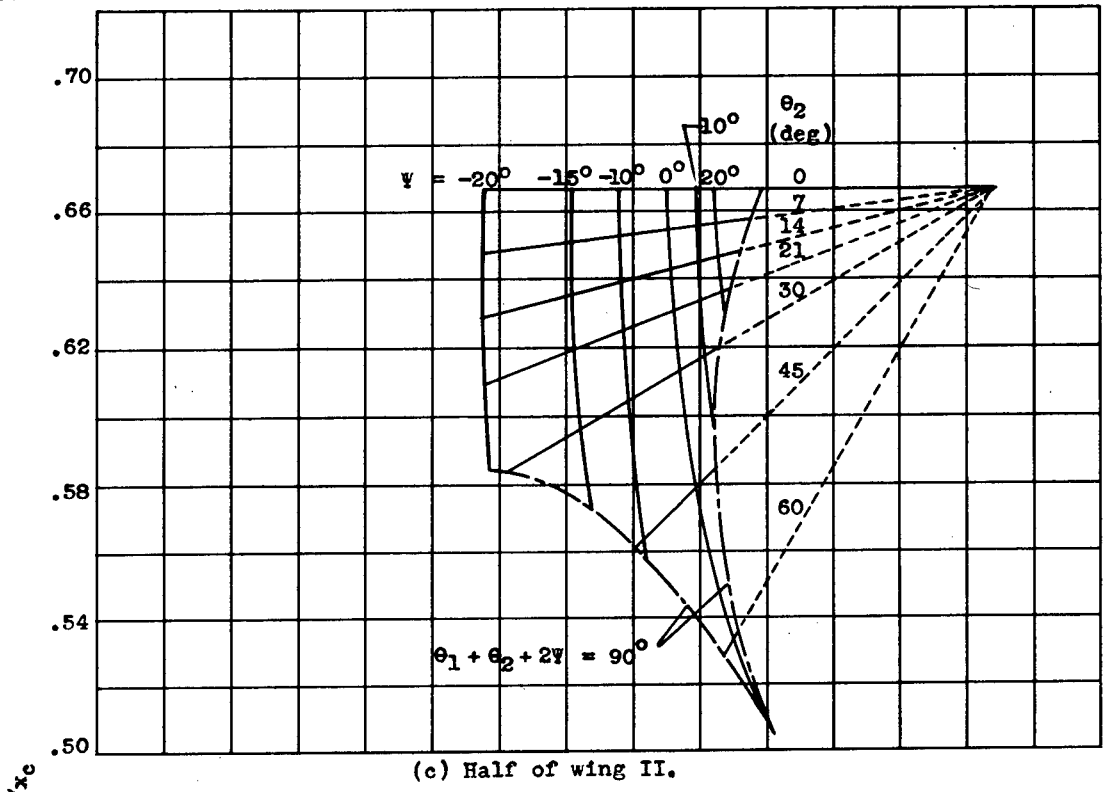

(c) Half of wing II.

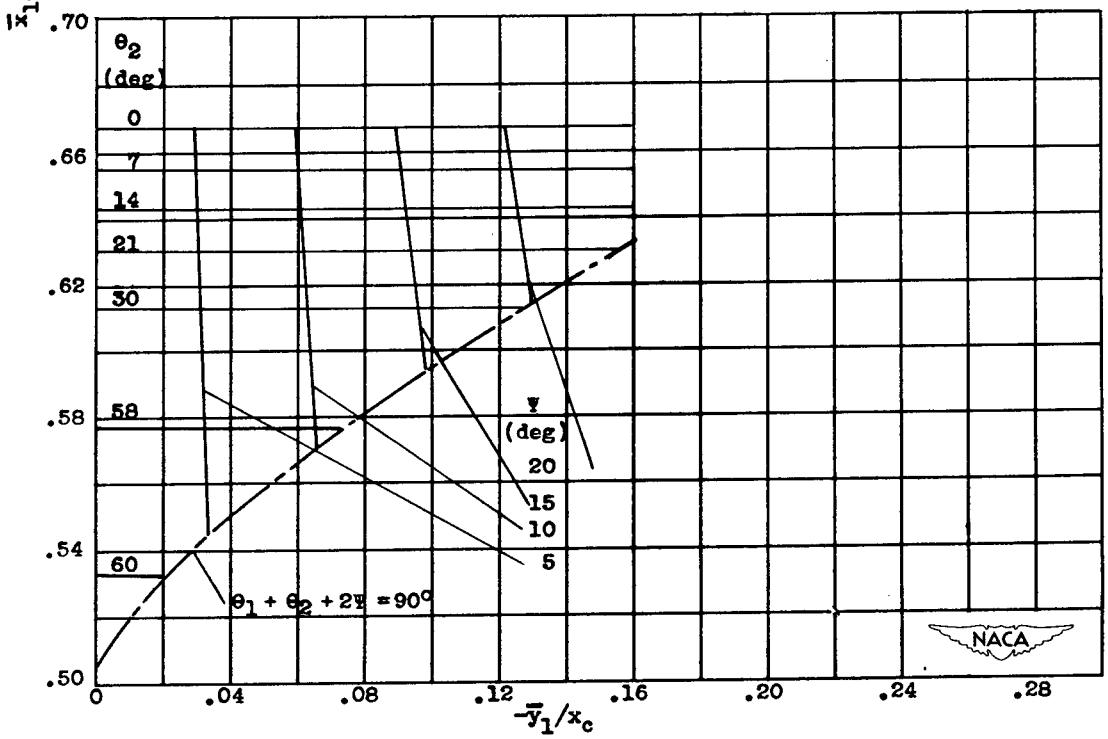

(d) Entire wing II.

Figure 6. - Continued. Variation of center of pressure with yaw angle and trailing-edge sweepback angle. $\theta_l = \tan^{-1} 0.4$.

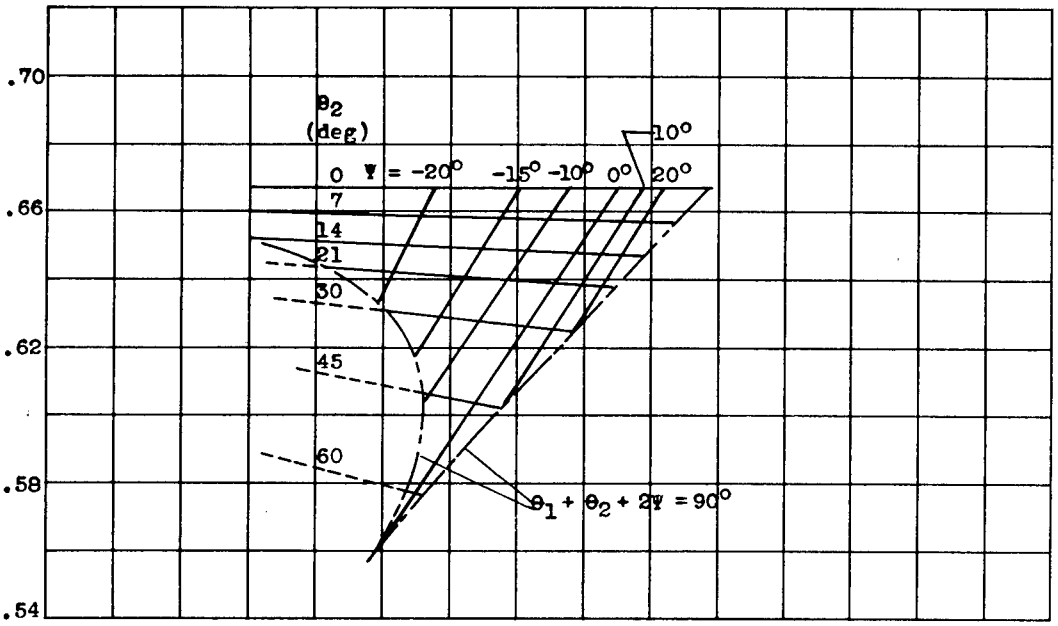

(e) Half of wing III.

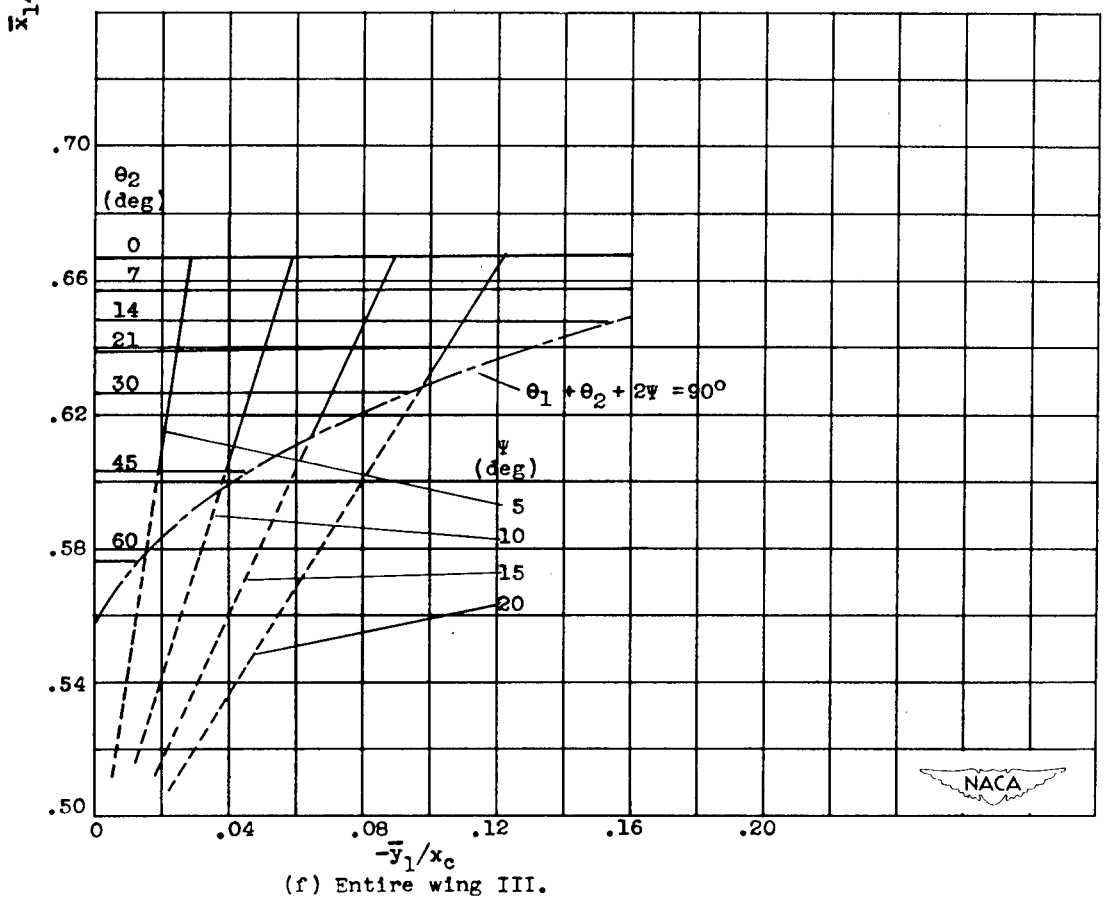

(f) Entire wing III.

Figure 6. - Concluded. Variation of center of pressure with yaw angle and trailing-edge sweepback angle. $\theta_1 = \tan^{-1} 0.4$.

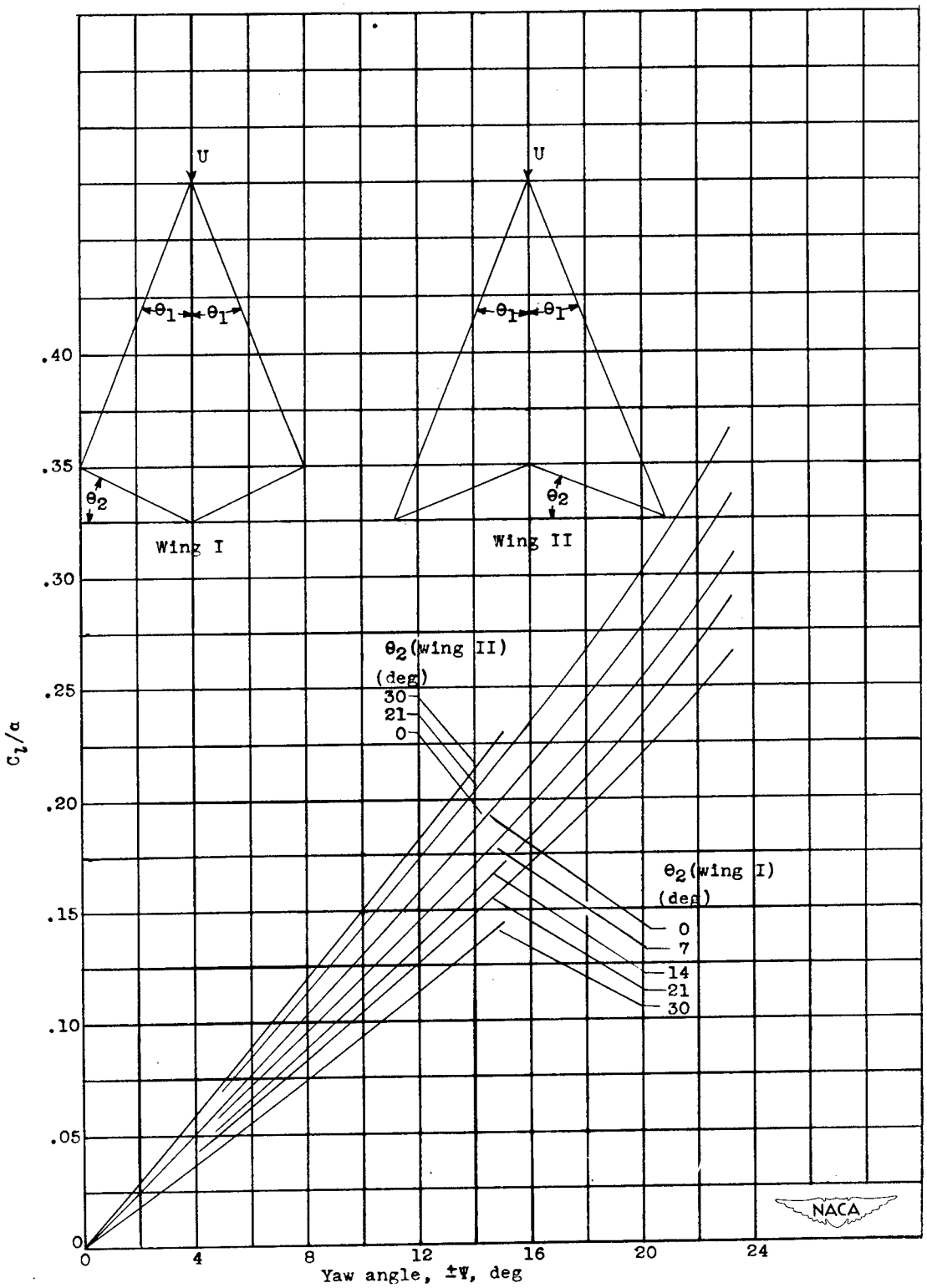

Figure 7. - Comparison of variation of rolling-moment coefficient with yaw and trailing-edge sweepback angle. $\theta_1 = \tan^{-1} 0.4$; $M = \sqrt{2}$.